

**Oxyplasma meridianum gen. nov., sp. nov., an extremely acidophilic organotrophic member of the order Thermoplasmatales**

Golyshina, Olga V; Lunev, Evgenii A; Distaso, Marco A; Bargiela, Rafael; Gaines, Matthew C; Daum, Bertram; Ferrer, Manuel; Bale, Nicole J; Koenen, Michel; Damsté, Jaap S Sinninghe; Yakimov, Mikhail M; Golyshin, Peter N

International Journal of Systematic Evolutionary Microbiology

DOI:

[10.1099/ijsem.0.006499](https://doi.org/10.1099/ijsem.0.006499)

Published: 27/08/2024

Peer reviewed version

[Cyswllt i'r cyhoeddiad / Link to publication](#)

Dyfyniad o'r fersiwn a gyhoeddwyd / Citation for published version (APA):

Golyshina, O. V., Lunev, E. A., Distaso, M. A., Bargiela, R., Gaines, M. C., Daum, B., Ferrer, M., Bale, N. J., Koenen, M., Damsté, J. S. S., Yakimov, M. M., & Golyshin, P. N. (2024). *Oxyplasma meridianum* gen. nov., sp. nov., an extremely acidophilic organotrophic member of the order Thermoplasmatales. *International Journal of Systematic Evolutionary Microbiology*, 74(8). <https://doi.org/10.1099/ijsem.0.006499>

Hawliau Cyffredinol / General rights

Copyright and moral rights for the publications made accessible in the public portal are retained by the authors and/or other copyright owners and it is a condition of accessing publications that users recognise and abide by the legal requirements associated with these rights.

- Users may download and print one copy of any publication from the public portal for the purpose of private study or research.
- You may not further distribute the material or use it for any profit-making activity or commercial gain
- You may freely distribute the URL identifying the publication in the public portal ?

Take down policy

If you believe that this document breaches copyright please contact us providing details, and we will remove access to the work immediately and investigate your claim.

1 *Oxyplasma meridianum* gen. nov. sp. nov., an extremely acidophilic organotrophic member of the
2 order *Thermoplasmatales*

3
4 Olga V. Golyshina¹, Evgenii A. Lunev¹, Marco A. Distaso¹, Rafael Bargiela^{1,2}, Matthew C. Gaines³,
5 Bertram Daum³, Manuel Ferrer², Nicole J. Bale⁴, Michel Koenen⁴, Jaap S. Sinninghe Damsté⁴,
6 Mikhail M. Yakimov⁵, Peter N. Golyshin¹

7 ¹Centre for Environmental Biotechnology, School of Environmental and Natural Sciences, Bangor
8 University, Bangor, UK

9 ²Instituto de Catalisis y Petroleoquimica (ICP), CSIC, Madrid, Spain

10 ³Living Systems Institute and Department of Biosciences, Faculty of Health and Life Sciences,
11 University of Exeter, Exeter, UK

12 ⁴Department of Marine Microbiology and Biogeochemistry, NIOZ Royal Netherlands Institute for
13 Sea Research, Texel, Netherlands

14 ⁵Institute of Polar Sciences, CNR, Messina, Italy

15 Correspondence: Olga V Golyshina, o.golyshina@bangor.ac.uk

16

17 **Abstract**

18 A mesophilic, hyperacidophilic archaeon, strain M1^T, was isolated from a rock sample from
19 Vulcano Island, Italy. Cells of this organism were cocci with an average diameter of 1 µm. Some
20 cells possessed filaments. The strain grew in the range of temperatures between 15 and 52°C and
21 pH 0.5-4.0 with growth optima at 40°C and pH 1.0. Strain M1^T was aerobic and
22 chemoorganotrophic, growing on complex substrates, such as casamino acids, trypticase, tryptone,
23 yeast and beef extracts. No growth at expenses of oxidation of elemental sulfur or reduced sulfur
24 compounds, pyrite, or ferrous sulfate was observed. The core lipids were glycerol dibiphytanyl
25 glycerol tetraether lipids (membrane spanning) with 0 to 4 cyclopentane moieties and archaeol, with
26 trace amounts of hydroxy archaeol. The dominant quinone was MK-7:7. The genome size of M1^T
27 was 1.67 Mbp with a G+C content of 39.76 mol%, and both characteristics were well within the
28 common range for *Thermoplasmatales*. The phylogenetic analysis based on 16S rRNA gene

29 sequence placed the strain M1^T within the order *Thermoplasmatales* with sequence identities of
30 90.9, 90.3 and 90.5% to the closest SSU rRNA gene sequences from organisms with validly
31 published names, *Thermoplasma acidophilum*, *T. volcanium* and *Thermogymnomonas acidicola*,
32 respectively. Based on the results of our genomic, phylogenomic, physiological and
33 chemotaxonomic studies, we propose strain M1^T (=DSM 116605 =JCM 36570) to represent a new
34 genus and species, *Oxyplasma meridianum* gen. nov., sp. nov., within the order *Thermoplasmatales*.

35

36 **Keywords:** *Oxyplasma*, *Thermoplasmatales*, geothermal environments, acidic environments,
37 acidophilic archaea

38

39 The GenBank accession number for the 16S rRNA gene strain of strain M1^T is OR949061. The
40 GenBank accession number for complete genome sequence of strain M1^T is CP133772.

41

42 **Introduction**

43 Archaea of the order *Thermoplasmatales* are ubiquitous across most terrestrial acidic environments
44 of various scale and origin (geothermal and anthropogenic sulfide-ores-containing mining biotopes
45 with temperatures between 10-60°C) [1-3]. These archaea occur in a variety of sites in significant
46 abundance, suggesting they contribute substantially to element cycling and community composition
47 [4-6]. However, most of these archaea were detected by obtaining metagenomes worldwide and,
48 thus, remain uncultured. Up to now, there are six genera with validly published names within the
49 order *Thermoplasmatales*: *Thermoplasma*, *Picrophilus*, *Ferroplasma*, *Thermogymnomonas*,
50 *Acidiplasma* and *Cuniculiplasma* [7]. The scarcity of isolated and described members limits our
51 knowledge about the ecological, physiological, morphological, and chemotaxonomic properties of
52 these organisms. The phylogenetic position of the order *Thermoplasmatales* has been recently
53 changed. Originally, the order was affiliated with the Phylum *Euryarchaeota* [2]. However, an
54 updated phylogenetic reconstruction from Genome Taxonomy Database (GTDB) firmly placed
55 these organisms as a separate Phylum *Thermoplasmata* [8, 9]. According to this classification, the
56 Phylum *Thermoplasmata* comprises classes “*Ca. Poseidonia*” and *Thermoplasmata*, with the
57 latter containing multiple orders along with *Thermoplasmatales*. The tight clustering of
58 *Thermoplasmatales* together with other orders into a separate phylum point at a distinct
59 evolutionary trajectory for this group of organisms. There are also other factors, making these
60 archaea particularly attractive for further isolation efforts and study. Archaea of the order

61 *Thermoplasmatales* are the most acidophilic organisms among prokaryotes, able to survive at pH
62 values lower than 0 [10]. Another hallmark is the lack of cell walls in most cultured members,
63 leading to a pleomorphic morphology, which is unusual for archaea [2]. Finally, these
64 hyperacidophilic archaea are an attractive target for bioprospecting of enzymes and metabolites of
65 biotechnological relevance [11-15].

66 In this study, we describe a new member of the order *Thermoplasmatales* isolated from a rock
67 sample of Vulcano Island, Italy. Based on the morphological, physiological, chemotaxonomic, and
68 phylogenetic characteristics, the organism represents a new genus and species within the order
69 *Thermoplasmatales*.

70

71 **Methods**

72 **Sampling, isolation and cultivation conditions**

73 The sampling was conducted in the Levante Bay of Vulcano Island (Aeolian archipelago, Italy;
74 38.416115° N, 14.96035° E) in October 2012. The collected sample was a soft biofilm on the
75 surface of the rock. For cultivation, the modified medium DSMZ 88 was used, which contained (g
76 l⁻¹): (NH₄)₂SO₄, 1.3; KH₂PO₄, 0.28; MgSO₄·7H₂O, 0.25; CaCl₂·2H₂O, 0.07; FeCl₃·6H₂O, 0.02.
77 Additionally, the medium was amended with the trace element solution SL-10 from DSMZ medium
78 320 in proportion 1:1000 (v/v), betaine at 0.06% (w/v) and vitamin solution Kao and Michayluk
79 (Sigma-Aldrich, Gillingham, UK) at 1:100 (v/v). Beef extract and tryptone (both ThermoFisher
80 Scientific, Paisley, UK), were added at final concentration 1 g l⁻¹. Casamino acids, trypticase, yeast
81 extract, amino acids, casein, chitin, cellulose, sucrose, lactose, raffinose, xylose, glucose and
82 galactose (all from ThermoFisher Scientific, Paisley, UK) were individually tested at a
83 concentration of 1 g l⁻¹. The pH of the medium was adjusted to 1.0-1.2 with concentrated H₂SO₄.
84 The oxidation of FeSO₄·7H₂O (25 g/l) and pyrite (Kremer Pigments, Aichstetten Germany; 1 g l⁻¹)
85 were tested in the medium DSMZ 874, as described previously, in the presence of yeast extract
86 (ThermoFisher Scientific Paisley, UK), 0.02% (w/v)) [16]. Reduced sulfur compounds, K₂S₄O₆ and
87 K₂S₂O₃ (both 5 mM), and elemental sulfur (Sigma Aldrich, Gillingham, UK, 1 g l⁻¹) were tested
88 separately in the DSMZ medium 88 in the presence of beef extract and tryptone (1 g l⁻¹). Anaerobic
89 growth with Fe₂(SO₄)₃ (10 mM) with and without yeast extract addition (0.02% w/v) was studied
90 in DSMZ media 88 and 874. Furthermore, the consumption of H₂ (1 and 5 ml taken by syringe from
91 gas phase) was tested with and without Fe₂(SO₄)₃ (10 mM) under anaerobic conditions in the DSMZ
92 medium 88. The growth under anaerobic conditions was studied also in the presence of elemental
93 sulfur (1 g l⁻¹), ferric citrate (1 mM) and KNO₃ (10 mM), and fermentative growth was tested in the

94 DSMZ medium 88 with addition of beef extract and tryptone (both in concentrations 1 g l⁻¹). The
95 gas mixture used for anaerobic atmosphere was N₂:H₂:CO₂, in proportion 80:10:10. The anaerobic
96 growth was studied in 18 ml Hungate type culture tubes with butyl rubber stoppers (Glasgerätebau
97 Ochs, Bovenden, Germany) with the volume of cultures between 5-15 ml and with the gas
98 headspace varied 3-13 ml. The pure culture was isolated by serial dilution to extinction method and
99 monitored by PCR amplification with universal bacterial (F27 and R1492) and archaeal (AF23 and
100 R1492) primers. The purified cultures were grown aerobically in 100 ml Erlenmeyer borosilicate
101 Duran® flasks (DWK Life Sciences GmbH, Mainz, Germany) for ca. 5 days with 25 ml of medium
102 with shaking at 120 rpm. The growth was studied at temperatures between 5 and 55°C and pH
103 between 0 and 4.5. The modified DSMZ Medium 88 with amendments described above and organic
104 substrates (beef extract and tryptone (both in concentrations 1 g l⁻¹)) with various pH values was
105 used for determining the optimal pH for growth. The growth was estimated spectrophotometrically
106 at the wavelength 600 nm in a BioPhotometer Plus (Eppendorf, Hamburg, Germany), and direct
107 cell counts in a Thoma chamber for anaerobic cultivation conditions.

108 **Cell morphology**

109 Cell morphology was investigated with the use of transmission electron microscopy (TEM). For
110 TEM, 5 µL of liquid cell culture was pipetted onto Cu 400 mesh Negative stain grids (Agar Scientist
111 AGS160-4). These grids had been glow discharged at 20 mA for 1 min and the biological sample
112 applied within 15 min after glow discharging. The sample was left on the grid for 2 min, before
113 excess liquid was blotted off from the periphery of the grid using filter paper (Whatman, Grade 1).
114 Three wash steps using Milli-Q water were performed, whereby 5 µL of Milli-Q was pipetted onto
115 the grid before being immediately removed using filter paper via the same blotting method. 1%
116 uranyl acetate stain (dissolved in Milli-Q) was then applied to the grid, before being immediately
117 blotted off. Finally, a second application of 1% uranyl acetate stain was pipetted onto the grid and
118 left for 30 sec before blotting. The grids were then left to dry on filter paper for 20 min before being
119 investigated in a Thermo Fisher Tecnai Spirit TEM, operating at 120 kV. Images were recorded
120 using a OneView CMOS detector (Gatan).

121 **Chemotaxonomic characterisation**

122 The intact polar lipids (IPLs) and quinones were extracted from freeze-dried biomass with
123 methanol, dichloromethane (DCM) and phosphate buffer (2:1:0.8, v:v:v) using an ultrasonic bath
124 (2 x 10 min). The extracts were phase-separated by adding DCM and buffer to a final solvent ratio
125 of 1:1:0.9 (v:v:v). The IPL-containing organic phases were re-extracted twice with DCM. All steps
126 of the extraction were then repeated on the freeze-dried biomass with a solvent mixture of methanol,

127 DCM and trichloroacetic acid pH 2-3 (2:1:0.8, v:v:v). Finally, the combined extract was dried under
128 a stream of N₂ gas [17]. For analysis, the extracts were redissolved in MeOH:DCM (9:1, v:v) and
129 filtered through 0.45 µm cellulose syringe filters (4 mm diameter; Grace Alltech, Deerfield, IL,
130 United States). Analysis was carried out using an Ultra High-Pressure Liquid Chromatography-
131 High Resolution Mass Spectrometry (UHPLC-HRMSⁿ) [17]. Identification was carried out by
132 comparison of accurate masses and mass spectral fragmentation with published data for IPLs and
133 for quinones [18-20].

134 **Genome sequencing, annotation and comparative genomic analysis**

135 The DNA was isolated using a QIAGEN DNeasy PowerLyzer PowerSoil Kit (QIAGEN, Hilden,
136 Germany) according to the manufacturer's protocol from 25-100 ml cultures and quantified using
137 QubitTM dsDNA BR Assay kit and Qubit fluorometer (Invitrogen, Carlsbad, CA, UK). The genome
138 was sequenced using in-house Illumina MiSeq and Nanopore platforms. Pre-processing of
139 Nanopore reads were conducted by porechop (<https://github.com/rrwick/Porechop>) and filtlong
140 (<https://github.com/rrwick/Filtlong>). The assembly was performed using the "zga" pipeline
141 (<https://github.com/laxeye/zga>) with Unicycler version 0.4.4. Genome annotation was performed
142 using PGAP v2022-12-13.build6494 [21] and the genome was submitted to GenBank with
143 accession number CP133772. Comparative genomic analysis was done using a dDDH (digital
144 DNA-DNA hybridisation) calculation, formula *d4* and Average Nucleotide Identity (ANIb and
145 ANIm), utilising the DSMZ platform (<https://tygs.dsmz.de>) and JSpeciesWS web server
146 (<https://jspecies.ribohost.com/jspeciesws/#analyse>), respectively [22, 23].

147 **Phylogenetic analysis**

148 For the phylogenetic analysis based on 16S rRNA gene sequence, reference sequences have been
149 downloaded from the NCBI nucleotide database and aligned using MAFFT v7 [24]. Multiple
150 alignment was trimmed using TrimAL 1.2rev59 [25] and the tree was performed by maximum
151 likelihood method with a bootstrap based on 1,000 replicates using the R package phangorn [26].
152 Graphical representation for both phylogenetic trees was developed using R programming language
153 [27] and the package ape [28]. Phylogenetic analysis based on 122 proteins alignment was
154 performed using GTDB-tk tool v2.1.1 [29].

155

156 **Results and Discussion**

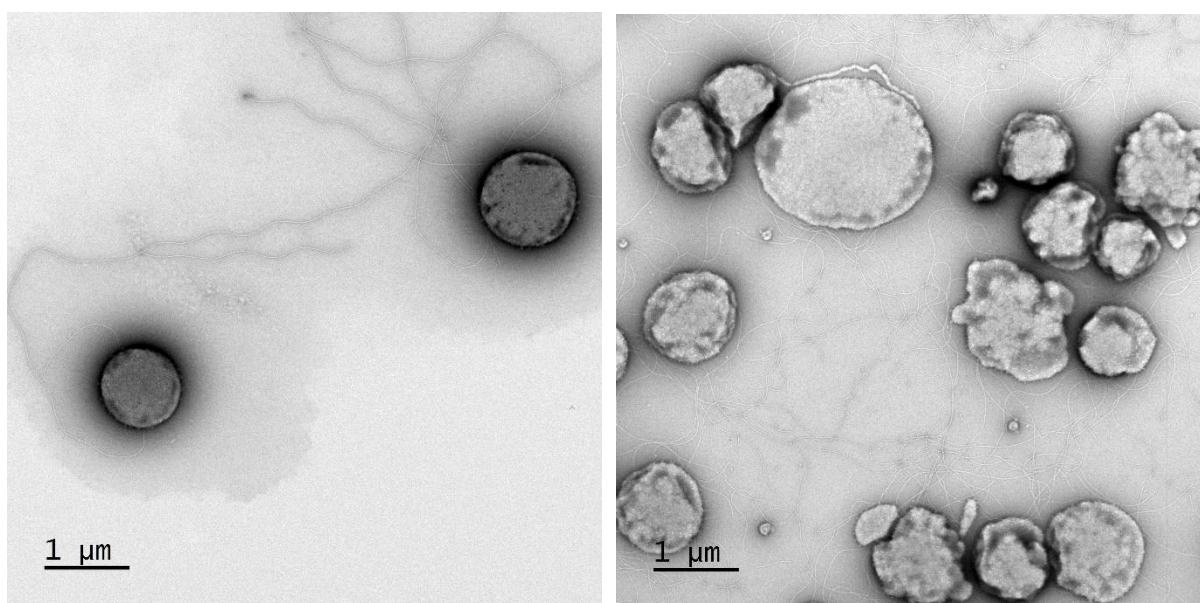
157 **Phenotypic properties**

158 Growth of the isolate M1^T occurred between 15 and 52°C with the optimum at 40°C (doubling time
159 19.2 h), reaching up to 7 x 10⁸ cells/ml. Growth occurred in a pH range between 0.5 and 4 with a
160 pH 1 being the optimal value. The highest growth rate as determined by optical density
161 measurements was detected with a mixture of beef extract and tryptone in a concentration of 1 g l⁻¹
162 each. The following substrates (1 g l⁻¹ each) were stimulating growth at optimal temperature and
163 pH: casamino acids, trypticase, yeast extract, with weak growth detected with amino acids. No
164 growth stimulation was observed with casein, chitin, cellulose, sucrose, lactose, raffinose, xylose,
165 glucose and galactose. No growth or stimulation of growth was observed with addition of elemental
166 sulfur or reduced sulfur compounds (tetrathionate or thiosulfate). No growth on ferrous iron sulfate
167 or pyrite was detected in the presence or absence of yeast extract. No fermentative growth, and no
168 anaerobic growth with any acceptors tested was observed.

169 Cell Morphology

170 Transmission electron micrographs revealed that cells had slightly irregular coccoid morphology
171 with an average diameter of ~1 μm (Fig. 1). The cells extended on average up to 3 surface filaments
172 per cell in early log phase. This value then increased to 8 surface filaments per cell in the late log
173 to stationary growth phases. These filaments closely resembled pili or archaella. In accordance with
174 previous observations of *Thermoplasmatales* species [2], no canonical S-layer was evident.
175 Notably, the cells were speckled with small (10-20 nm) globular surface structures (Fig. 1). Close
176 inspection of these extensions did not reveal any similarity to viruses and indeed, viral DNA was
177 absent in the culture.

178



179

180 **Fig. 1 (a and b)**

181 **Chemotaxonomy**

182 For lipid analysis three separate culture of strain M1^T were grown and harvested at the late log
 183 phase. The most abundant core lipids (ca. 80%) were glycerol dibiphytanyl glycerol tetraether lipids
 184 (GDGTs, membrane spanning) with 0 to 4 cyclopentane moieties (GDGT-0 – GDGT-4). The most
 185 dominant GDGTs were GDGT-2 and GDGT-4 (Table 1). A similar GDGT distribution was
 186 observed for the (hyper)acidophiles “*Ferroplasma acidarmanus*” [30], *Thermogymnomonas*
 187 *acidicola* [31], *Thermoplasma acidophilum* [32], *Acidiplasma aeolicum* [16], *C. divulgatum* [7], all
 188 also belonging to the order *Thermoplasmatales*. The majority of GDGT IPLs had a phosphoglycerol
 189 (PG) head group at one glycerol moiety, with predominantly 1, and to a minor extent, 2-3 hexose
 190 sugar(s) (glycosyl; gly) at the other glycerol moiety (Table 2). Archaeol (AR) and minor amounts
 191 of hydroxy archaeol (OH-AR) represented the other 20% of the core lipids. PG was the only polar
 192 head group of AR detected, whilst OH-AR was only detected with a DiGly head group. The
 193 dominant (ca. 94%) quinone present in M1^T was MK-7:7 (Table 2).

194

195 **Table 1.** Intact polar lipids identified in *Oxyplasma meridianum* strain M1^T and their relative
 196 abundance (in percent of lipid peak area). Columns 1-3 represent the data of the three parallel
 197 cultures.

Polar Headgroup 1	Polar Headgroup 2	Core	[M+H] ⁺	AEC	Δ mmu	Relative abundance (%)		
						1	2	3
None		AR	653.680	C ₄₃ H ₈₉ O ₃	0.3	6.3	6.6	8.8
PG		AR	807.683	C ₄₆ H ₉₆ O ₈ P	0.9	9.3	9.4	11.3
DiGly		OH-AR	993.781	C ₅₅ H ₁₀₉ O ₁₄	0.0	3.1	3.2	3.6
PG		GDGT-0	1456.325	C ₈₉ H ₁₈₀ O ₁₁ P	1.0	0.5	1.4	0.4
		GDGT-1	1454.309	C ₈₉ H ₁₇₈ O ₁₁ P	0.8	0.3	0.8	0.3
		GDGT-2	1452.293	C ₈₉ H ₁₇₆ O ₁₁ P	1.5	6.6	8.8	5.8
		GDGT-3	1450.278	C ₈₉ H ₁₇₄ O ₁₁ P	1.3	1.9	2.0	1.5
		GDGT-4	1448.262	C ₈₉ H ₁₇₂ O ₁₁ P	1.5	5.6	4.1	4.4
		Total				15	17	13
PG	Gly	GDGT-0	1618.378	C ₉₅ H ₁₉₀ O ₁₆ P	0.9	0.3	1.1	0.4
		GDGT-1	1616.352	C ₉₅ H ₁₈₈ O ₁₆ P	12	2.3	3.7	2.4
		GDGT-2	1614.348	C ₉₅ H ₁₈₆ O ₁₆ P	0.2	11.2	15.8	10.3
		GDGT-3	1612.323	C ₉₅ H ₁₈₄ O ₁₆ P	9	6.8	7.9	6.2
		GDGT-4	1610.317	C ₉₅ H ₁₈₂ O ₁₆ P	0.7	42.9	32.6	41.0
		Total				64	61	60
PG	diGly	GDGT-0	1780.429	C ₁₀₁ H ₂₀₀ O ₂₁ P	2.2	0.1	0.2	0.2
		GDGT-1	1778.412	C ₁₀₁ H ₁₉₈ O ₂₁ P	3.4	0.0	0.1	0.1
		GDGT-2	1776.399	C ₁₀₁ H ₁₉₆ O ₂₁ P	0.7	1.5	1.5	1.8
		GDGT-3	1774.382	C ₁₀₁ H ₁₉₄ O ₂₁ P	2.8	0.2	0.2	0.3
		GDGT-4	1772.367	C ₁₀₁ H ₁₉₂ O ₂₁ P	2.2	0.6	0.3	0.7
		Total				2	2	3
PG	triGly	GDGT-0	1942.479	C ₁₀₇ H ₂₁₀ O ₂₆ P	4.9	0.1	0.2	0.2
		GDGT-1	1940.468	C ₁₀₇ H ₂₀₈ O ₂₆ P	0.6	0.0	0.1	0.1

GDGT-2	1938.451	C ₁₀₇ H ₂₀₆ O ₂₆ P	2.1	0.5	0.5	0.6
GDGT-3	1936.434	C ₁₀₇ H ₂₀₄ O ₂₆ P	2.9	0.1	0.1	0.2
GDGT-4	1934.420	C ₁₀₇ H ₂₀₂ O ₂₆ P	1.5	0.2	0.2	0.4
Total				1	1	1
Sum AR				16	16	20
Sum OH-AR				3	3	4
GDGT-0				1	3	1
GDGT-1				3	5	3
GDGT-2				20	27	19
GDGT-3				9	10	8
GDGT-4				49	37	46

198 Δ mmu = (measured mass – calculated mass) x 1000 as calculated for strain 1; AEC = assigned elemental
 199 composition; PG = phosphatidylglycerol; Gly = monoglycosyl; diGly = diglycosyl; triGly = triglycosyl; AR =
 200 archaeol; OH-AR = hydroxy archaeol, GDGT = glycerol dibiphytanyl glycerol tetraether.

201
 202 **Table 2.** Menaquinones identified in *Oxyplasma meridianum* M1^T. 1-3 are data of three parallel
 203 cultures of strain M1^T.

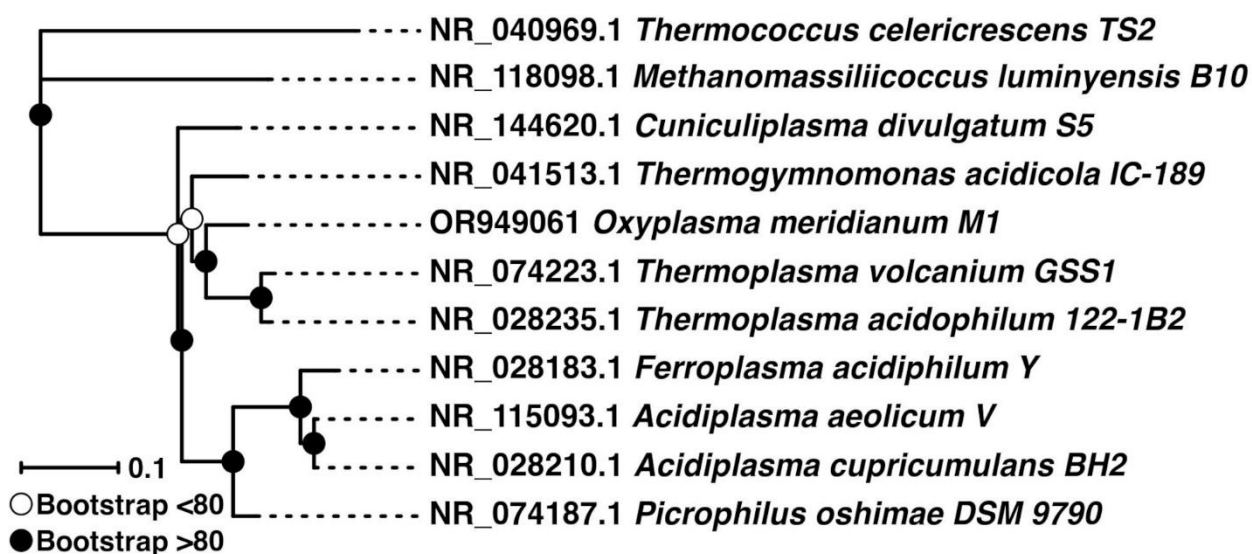
	[M+H] ⁺	AEC	Δ mmu	Relative abundance (%)		
				1	2	3
MK-8:8	717.560	C ₅₁ H ₇₃ O ₂	0.2	1.1	1.1	1.1
MK-7:7	649.498	C ₄₆ H ₆₅ O ₂	0.3	94.2	93.2	94.6
MK-7:6	651.514	C ₄₆ H ₆₇ O ₂	0.2	4.7	5.6	4.3

204 Δ mmu = (measured mass – calculated mass) x 1000 as calculated for strain 1; AEC = assigned elemental
 205 composition.

207 Phylogenetic analysis

208 Based on its 16S rRNA gene sequence, the strain M1^T clusters together with other archaea of the
 209 order *Thermoplasmatales*, class *Thermoplasmata*, phylum *Thermoplasmata*. The nearest
 210 phylogenetic neighbour of the strain M1^T is *Thermoplasma acidophilum* (90.9%), followed by
 211 *Thermogymnomonas acidicola* (90.5%) and *Thermoplasma volcanium* (90.3%) (Fig. 2). Therefore,
 212 according to the accepted boundaries for a genus (<94.5% for 16S rRNA gene sequence identity)
 213 [33] M1^T represents a new genus.

214



216

217 **Fig. 2**

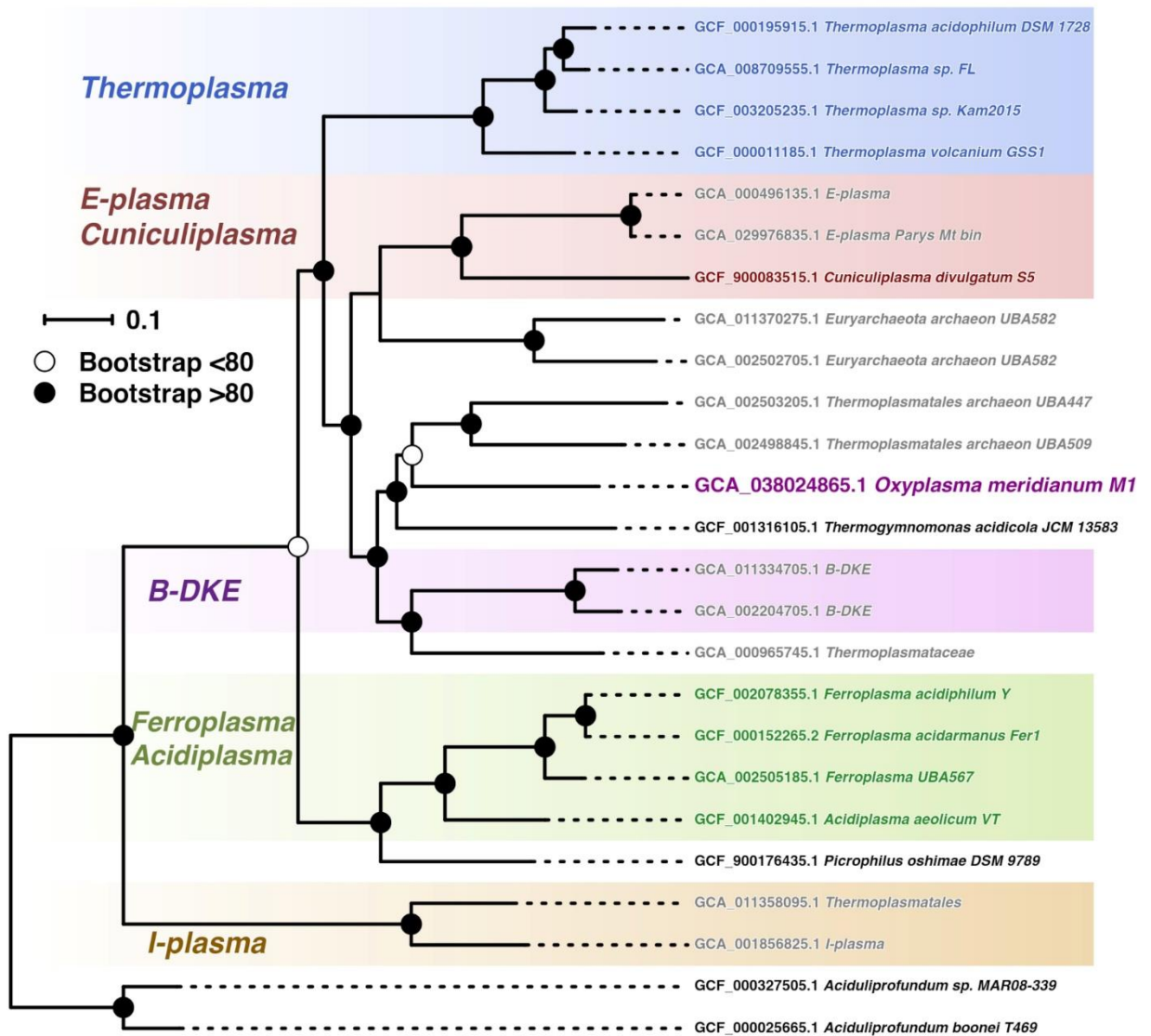
218

219 **Genome properties**

220 About 239.2-fold genome coverage by Illumina reads and 23.4-fold coverage by Oxford Nanopore
 221 reads were obtained. The genome assembly resulted in one circular chromosome of 1.67 Mbp with
 222 a G+C content 39.76%. The genome annotation revealed 1725 genes with 1679 protein-coding
 223 sequences and 43 genes encoding tRNA. Analysis of the genome revealed the presence of all
 224 enzymes required for glycolysis. Genes encoding the non-phosphorylative Entner-Doudoroff
 225 pathway and the non-oxidative pentose phosphate pathway were detected. We also identified all
 226 genes encoding the TCA cycle in the genome with alpha-ketoglutarate dehydrogenase as the only
 227 exception (Table S1). Likely, the function of this enzyme is performed by 2-oxoacid:acceptor
 228 oxidoreductase. Multiple copies of genes are present in the genome, including a location in close
 229 proximity to the TCA enzymes-encoding genes. This possibility was previously considered for
 230 other organisms, including a phylogenetic neighbour of the strain M1^T, *P. torridus* [34]. Aerobic
 231 respiration was backed up by the presence of genes encoding a NADH dehydrogenase complex, a
 232 cupredoxin-domain-containing (plastocyanin) protein, a cytochrome *cbb3*-type cytochrome C
 233 oxidase subunits I and II, and a polyferredoxin NapH superfamily (OXIME_000996 –
 234 OXIME_001001). Furthermore, cytochrome ubiquinol/*bd* terminal oxidase subunits I and II and
 235 cytochrome bc complex cytochrome b subunit encoding genes (OXIME_001706 - OXIME_001707
 236 and OXIME_000377) were identified in the genome. Moreover, we detected V-type ATP synthase
 237 subunits A, B, C, D, F, E and H in the genome of the strain M1^T. Genes for proteolytic proteins
 238 affiliated to peptidase families M50, M13, M19, and S49, a trypsin-like peptidase, an archaeal Lon

239 protease, a tricorn protease, and a thermopsin were found in the genome and reflect the
240 organotrophic lifestyle of the strain M1^T. We detected genes encoding a mevalonate 3-kinase, a
241 mevalonate 3-phosphate 5-kinase and mevalonate biphosphate decarboxylase proteins, confirming
242 the route III of the mevalonate pathway, characteristic for *Thermoplasmatales* archaea [35-37].
243 Interestingly, we also identified genomic loci for hercynine oxygenase/ergothioneine biosynthesis
244 protein EgtB (OXIME_001566) and a L-histidine N(alpha)-methyltransferase (OXIME_001567),
245 both being involved into the ergothioneine pathway. Ergothioneine is a low molecular weight thiol,
246 a derivative of histidine with a sulfur atom containing imidazole ring and was previously predicted
247 in some archaeal genomes considering that it might be synthesised in archaea [38]. The organism
248 encodes the CRISPR-Cas (Clusters of Regularly Interspaced Short Palindromic Repeats)-associated
249 proteins, namely co-localised genes encoding for endoribonucleases Cas2 and Cas6, an
250 endonuclease Cas2, type I_D protein Cas5/Csc1, Csc2, Cas4 and two copies of endonuclease Cas1
251 genes. To summarise, physiological, morphological and genomic features of the strain M1^T suggest
252 this organism to be a typical member of the order *Thermoplasmatales* (Table 3).

253 The phylogenetic tree based on 122 concatenated proteins revealed that the M1^T strain is the closest
254 to *Thermogymnomonas acidicola* among organisms with validly published names and most similar
255 metagenome assembled genomes (Fig. 3).



257
258 **Fig. 3**

259
260 dDDH (formula $d4$) showed values significantly below the threshold level of 70% and ANI
261 calculations produced indices lower than 95-96% for strains M1 and *Thermoplasmatales* archaea
262 with validly published names (Tables S2 and S3), recommended for species delineation [39].

263 **Table 3.** Main characteristics of genera of the order *Thermoplasmatales* with validly published
264 names and strain M1^T.

Characteris tic	<i>Thermo plasma</i>	<i>Picrophilus</i>	<i>Ferroplasma</i>	<i>Acidiplasma</i>	<i>Thermogymno monas</i>	<i>Cuniculi plasma</i>	M1 ^T
	1	2	3	4	5	6	

Cell wall/S-layer	-	+	-	-	-	-	-
Growth temperature, °C							
Range	33-69	47-65	15-45	15/22-65	38-68	10-48	15-52.5
Optimum	67	60	35-37	45-53.5	60	37-40	40
Growth pH							
Range	0.5-4	0-3.5	1.3-2.2	0/0.4-1.8/4	1.8-4	0.5-4	0.5-4
Optimum	1-2	0.7	1.7	1-1.6	3	1-1.2	1
Fe ²⁺ oxidation	-	-	+	+	-	-	-
Anaerobic growth	+	-	±	+	-	+	-
DNA G+C content (mol%)	38-46	36	37	34-36	56	37	40

265 Data taken from: [7, 10, 16, 31, 40-42].

266

267 Conclusion

268 The strain M1^T is a mesophilic, thermotolerant, hyperacidophilic, aerobic, organotrophic and cell-
269 wall lacking organism. The physiology of the organism is comparable to representatives of all
270 genera of *Thermoplasmatales* with validly published names characterised up to date, which reflects
271 the adaptation to specific physicochemical conditions of indigenous environments. The inability of
272 anaerobic metabolism resembles that of *Picrophilus* and *Thermogymnomonas*, both of which were
273 isolated from geothermal settings as well [10, 31]. Electron microscopy suggested the lack of cell
274 wall, which is also common in *Thermoplasmatales* [2, 7]. Interestingly, the majority of cells had
275 relatively small sizes (<1 µm) and possessed multiple (up to 8) filaments. The membrane lipid
276 composition of M1^T was found to be rather characteristic for this group of archaea, with core lipids
277 (GDGTs and archaeol) content being generally similar to that in *C. divulgatum*, which has a similar
278 pH and temperature range, and both having menaquinone MK 7:7 as the main quinone [7]. The
279 genome of the strain M1^T had size and G+C molar content rather typical for all known
280 *Thermoplasmatales* and encoded proteins essential for aerobic and peptidolytic lifestyle. It should
281 be noted that the GenBank records on 16S rRNA sequences of organisms with identities >98% to
282 the strain M1^T are represented by acidic environments of geothermal origin and mining regions, e.g.
283 GenBank accession numbers, AF544219 (Iron Mountain acid mine drainage site, California, USA),
284 KJ907756 (Michoacan, Los Azufres thermal and acidic green biofilms from a fumarole, Mexico),
285 DQ303253 and EF441883 (floating microscopic filaments from Rio Tinto and endolithic

286 community in the basin of Rio Tinto, Spain), and KM410353 (biofilm from subsurface sulfidic cave
287 stream, Italy). These results imply that representatives of the *Oxyplasma* genus similarly to
288 phylogenetic neighbours forming the same order, are distributed across the globe in ecological
289 niches with low pH and diverse temperatures and might be both non-thermophilic and moderately
290 thermophilic organisms, the known property for other *Thermoplasmatales* [7]. Based on the
291 polyphasic (genomic and phylogenomic, chemotaxonomic and physiological) analysis, strain M1^T
292 is proposed to represent a novel genus and species with the name *Oxyplasma meridianum* gen. nov.,
293 sp. nov. within the family *Thermoplasmataceae*, order *Thermoplasmatales*.

294

295 **Description of *Oxyplasma* gen. nov.**

296 *Oxyplasma* (O.xy.plas'ma. Gr. masc. adj. *oxys*, acid; Gr. neut. n. *plasma*, something shaped or
297 moulded, N.L. neut.n.).

298 *Oxyplasma* a form living in acid.

299 Cells are lacking cell walls. Aerobic, mesophilic/thermotolerant. Organotrophic. Hyperacidophilic.

300 The core lipids: archaeol with trace amounts of hydroxy archaeol and glycerol dibiphytanyl
301 glycerol tetraether lipids. The dominant Quinone MK-7:7.

302 The type species is *Oxyplasma meridianum*.

303 **Description of *Oxyplasma meridianum* sp. nov.**

304 *Oxyplasma meridianum* (me.ri.di.a'num L.neut.adj. *meridianum*, southern, isolated from the South
305 of Italy).

306 Cells are regular and irregular cocci about 1 µm in diameter. The temperature range for growth
307 (15-52.5°C), the optimum at 40°C. The pH range for growth (0.5-4), with an optimum at pH 1.

308 Grows organotrophically with tryptone, beef and yeast extracts, casamino acids, trypticase. Lipids
309 represented mostly by archaeol with trace amounts of hydroxy archaeol and glycerol dibiphytanyl
310 glycerol tetraether lipids (GDGT) with 0 to 4 cyclopentane moieties (GDGT-0 – GDGT-4). The
311 main respiratory quinone represented by menaquinone.

312 The type strain is M1^T (DSM 116605^T=JCM 36570^T), isolated from rock sample of Vulcano
313 Island, Italy. The DNA G+C content of type strain is 39.76 mol%. Accession numbers of the
314 strain M1^T 16S rRNA gene is OR949061 and of the complete genome is CP133772.

315

316 **Funding information**

317 PNG is indebted to the Era-Net Project ‘MetaCat’ funded through BBSRC, Contract Nr
318 BB/M029085/1. RB, PNG and OVG also acknowledge the support of the Centre for Environmental
319 Biotechnology Project N 810280, funded by the European Regional Development Fund (ERDF)
320 via the Welsh Government. MF acknowledges Ministerio de Ciencia e Innovación, AEI (DOI
321 10.13039/501100011033), FEDER and NextGenerationEU/PRTR (PID2020-112758RB-I00,
322 PDC2021-121534-I00, TED2021-130544B-I00).

323 **Conflicts of interest**

324 The authors declare no conflicts of interest.

325 **Data availability statement**

326 The GenBank accession number for complete genome sequence of *Oxyplasma meridianum* M1^T is
327 CP133772.

328

329 **References**

- 330 1. **Golyshina OV.** Environmental, biogeographic, and biochemical patterns of archaea of the
331 family *Ferroplasmaceae*. *Appl Environ Microbiol* 2011;77(15):5071-5078.
- 332 2. **Huber H, Stetter KO.** Thermoplasmatales. In: Dworkin, M., Falkow, S., Rosenberg, E.,
333 Schleifer, K.H., Stackebrandt, E. (eds) *The Prokaryotes*. New York; Springer, 2006.
334 https://doi.org/10.1007/0-387-30743-5_7.
- 335 3. **Mendez-Garcia C, Pelaez AI, Mesa V, Sanchez J, et al.** Microbial diversity and
336 metabolic networks in acid mine drainage habitats. *Front Microbiol* 2015;6:475.
- 337 4. **Arce-Rodríguez A, Puente-Sánchez F, Avedaño R, Martínez-Cruz M, et al.**
338 *Thermoplasmatales* and sulfur-oxidizing bacteria dominate the microbial community at the
339 surface water of a CO₂-rich hydrothermal spring located in Tenorio Volcano National
340 Park, Costa Rica. *Extremophiles* 2019;23(2):177-187.
- 341 5. **Korzhenkov AA, Toshchakov SV, Bargiela R, Gibbard H et al.** Archaea dominate the
342 microbial community in an ecosystem with low-to-moderate temperature and extreme
343 acidity. *Microbiome* 2019;7(1):11.
- 344 6. **Distaso MA, Bargiela R, Brailsford FL, Williams GB, et al.** High representation of
345 archaea across all depths in oxic and low-pH sediment layers underlying an acidic stream.
346 *Front Microbiol* 2020;11:576520.
- 347 7. **Golyshina OV, Lünsdorf H, Kublanov IV, Goldenstein NI, et al.** The novel extremely
348 acidophilic, cell-wall-deficient archaeon *Cuniculiplasma divulgatum* gen. nov., sp. nov.

- 349 represents a new family, *Cuniculiplasmataceae* fam. nov., of the order *Thermoplasmatales*.
350 *Int J Syst Evol Microbiol* 2016;66(1):332-40.
- 351 8. **Chuvochina M, Mussig AJ, Chaumeil PA, Skarszewski, A et al.** Proposal of names for
352 329 higher rank taxa defined in the Genome Taxonomy Database under two prokaryotic
353 codes. *FEMS Microbiol Lett* 2023;17:370:fnad071.
- 354 9. **Oren A, Göker M.** Validation List no. 215. Valid publication of new names and new
355 combinations effectively published outside the IJSEM. *Int J Syst Evol Microbiol*
356 2024;74(1):doi: 10.1099/ijsem.0.006173.
- 357 10. **Schleper C, Puehler G, Holz I, Gambacorta A, et al.** *Picrophilus* gen. nov., fam. nov.: a
358 novel aerobic, heterotrophic, thermoacidophilic genus and family comprising archaea
359 capable of growth around pH 0. *J Bacteriol* 1995;177:7050-7059.
- 360 11. **Rossoni L, Hall SJ, Eastham G, Licence P, Stephens G.** The putative mevalonate
361 diphosphate decarboxylase from *Picrophilus torridus* is in reality a mevalonate-3-kinase
362 with high potential for bioproduction of isobutene. *Appl Environ Microbiol*
363 2015;81(7):2625-2634.
- 364 12. **Murphy J, Walsh G.** Purification and characterization of a novel thermophilic β -
365 galactosidase from *Picrophilus torridus* of potential industrial application. *Extremophiles*
366 2019;23(6):783-792.
- 367 13. **Nagy I, Knispel RW, Kofler C, Orsini M, et al.** Lipoprotein-like particles in a
368 prokaryote: quinone droplets of *Thermoplasma acidophilum*. *FEMS Microbiol Lett*
369 2016;363(18):fnw169.
- 370 14. **Lund S, Courtney T, Williams GJ.** Probing the substrate promiscuity of isopentenyl
371 phosphate kinase as a platform for hemiterpene analogue production. *Chembiochem*.
372 2019;20(17):2217-2221.
- 373 15. **Rennella E, Huang R, Yu Z, Kay LE.** Exploring long-range cooperativity in the 20S
374 proteasome core particle from *Thermoplasma acidophilum* using methyl-TROSY-based
375 NMR. *Proc Natl Acad Sci USA* 2020;117:5298-5309.
- 376 16. **Golyshina OV, Yakimov MM, Lünsdorf H, Ferrer M, et al.** *Acidiplasma aeolicum* gen.
377 nov., sp. nov., a euryarchaeon of the family *Ferroplasmaceae* isolated from a
378 hydrothermal pool, and transfer of *Ferroplasma cupricumulans* to *Acidiplasma*
379 *cupricumulans* comb. nov. *Int J Syst Evol Microbiol* 2009;59:2815-2823.
- 380 17. **Bale NJ, Ding S, Hopmans EC, Arts MGI, et al.** Lipidomics of environmental microbial
381 communities. I: visualization of component distributions using untargeted analysis of high-
382 resolution mass spectrometry data. *Front Microbiol* 2021;12:659302.

- 383 18. **Yoshinaga MY, Kellermann MY, Rossel PE, Schubotz F, et al.** Systematic
384 fragmentation patterns of archaeal intact polar lipids by high-performance liquid
385 chromatography/electrospray ionization ion-trap mass spectrometry. *Rapid Commun Mass*
386 *Spectrom* 2011;25:3563–3574.
- 387 19. **Bale NJ, Sorokin DY, Hopmans EC, Koenen M, et al.** New insights into the polar lipid
388 composition of extremely halo(alkali)philic euryarchaea from hypersaline lakes. *Front*
389 *Microbiol* 2019;10:377.
- 390 20. **Elling FJ, Becker KW, Könneke M, Schröder JM, et al.** Respiratory quinones in
391 Archaea: phylogenetic distribution and application as biomarkers in the marine
392 environment. *Environ Microbiol* 2016;18:692–707.
- 393 21. **Tatusova T, DiCuccio M, Badretdin A, Chetvernin V, et al.** NCBI prokaryotic genome
394 annotation pipeline. *Nucl Acids Res* 2016;44(14):6614-6624.
- 395 22. **Meier-Kolthoff JP, Göker M.** TYGS is an automated high-throughput platform for state-
396 of-the-art genome-based taxonomy. *Nat Commun* 2019;10:2182.
- 397 23. **Richter M, Rosselló-Móra R, Glöckner FO, Peplies J.** JSpeciesWS: a web server for
398 prokaryotic species circumscription based on pairwise genome comparison. *Bioinformatics*
399 2015; pii: btv681.
- 400 24. **Katoh K, Standley DM.** MAFFT multiple sequence alignment software version 7:
401 improvements in performance and usability. *Mol Biol Evol* 2013;30(4):772-80.
- 402 25. **Capella-Gutierrez S, Silla-Martinez JM, Gabaldon T.** trimAl: a tool for automated
403 alignment trimming. *Bioinformatics* 2009;25:1972-1973.
- 404 26. **Schliep K.** phangorn: phylogenetic analysis in R. *Bioinformatics* 2011;27(4):592–593.
- 405 27. **R Core Team.** 2022. R: A language and environment for statistical computing. R
406 Foundation for Statistical Computing, URL: <https://www.R-project.org/>.
- 407 28. **Paradis E, Schliep K.** ape 5.0: an environment for modern phylogenetics and
408 evolutionary analyses in R. *Bioinformatics* 2019;35:526-528.
- 409 29. **Chaumeil P-A, Mussig AJ, Hugenholtz P, Parks DH.** GTDB-Tk v2: memory friendly
410 classification with the genome taxonomy database. *Bioinformatics* 2022;38:5315-5316.
- 411 30. **Macalady JL, Vestling MM, Baumler D, Boekelheide N, et al.** Tetraether-linked
412 membrane monolayers in *Ferroplasma* spp: a key to survival in acid. *Extremophiles*
413 2004;8:411-419.
- 414 31. **Itoh T, Yoshikawa N, Takashina T.** *Thermogymnomonas acidicola* gen. nov., sp. nov., a
415 novel thermoacidophilic, cell wall-less archaeon in the order *Thermoplasmatales*, isolated
416 from a solfataric soil in Hakone, Japan. *Int J Syst Evol Microbiol* 2007;57:2557-2561.

- 417 32. **Shimada H, Nemoto N, Shida Y, Oshima T, Yamagishi A.** Effects of pH and
418 temperature on the composition of polar lipids in *Thermoplasma acidophilum* HO-62. *J*
419 *Bacteriol* 2008;190(15):5404-5411.
- 420 33. **Yarza P, Yilmaz P, Pruesse E, Glöckner FO, et al.** Uniting the classification of cultured
421 and uncultured bacteria and archaea using 16S rRNA gene sequences. *Nat Rev Microbiol*
422 2014;12(9):635-645.
- 423 34. **Fütterer O, Angelov A, Liesegang H, Gottschalk G, et al.** Genome sequence of
424 *Picrophilus torridus* and its implications for life around pH 0. *Proc Natl Acad Sci USA*
425 2004;101(24):9091-9096.
- 426 35. **Azami Y, Hattori A, Nishimura H, Kawaide H, et al.** (R)-mevalonate 3-phosphate is an
427 intermediate of the mevalonate pathway in *Thermoplasma acidophilum*. *J Biol Chem*
428 2014;89(23):15957-15967.
- 429 36. **Vinokur JM, Cummins MC, Korman TP, Bowie JU.** An Adaptation to life in acid
430 through a novel mevalonate pathway. *Sci Rep* 2016;6:39737.
- 431 37. **Hoshino Y, Villanueva L.** Four billion years of microbial terpenome evolution. *FEMS*
432 *Microbiol Rev* 2023;47(2):1-39.
- 433 38. **Rawat M, Maupin-Furlow JA.** Redox and thiols in archaea. *Antioxidants* (Basel)
434 2020;9(5):381.
- 435 39. **Goris J, Konstantinidis KT, Klappenbach JA, Coenye T, et al.** DNA-DNA
436 hybridization values and their relationship to whole-genome sequence similarities. *Int J*
437 *Syst Evol Microbiol* 2007;57:81-91.
- 438 40. **Darland G, Brock TD, Samsonoff W, Conti SF.** A thermophilic acidophilic *Mycoplasma*
439 isolated from a coal refuse pile. *Science* 1970;170:1416-1418.
- 440 41. **Segerer A, Langworthy TA, Stetter KO.** *Thermoplasma acidophilum* and
441 *Thermoplasma volcanium* sp. nov. from solfatara fields. *Syst Appl Microbiol* 1986;10:161-
442 171.
- 443 42. **Golyshina OV, Pivovarova,TA, Karavaiko GI, Kondratéva TF, et al.** *Ferroplasma*
444 *acidiphilum* gen. nov., sp. nov., an acidophilic, autotrophic, ferrous-iron-oxidizing, cell-
445 wall-lacking, mesophilic member of the *Ferroplasmaceae* fam. nov., comprising a distinct
446 lineage of the *Archaea*. *Int J Syst Evol Microbiol* 2000;50:997-1006.

447

448 **Figure legends:**

449 **Figure 1 (a and b).** Negative stain transmission electron microscopy of strain M1^T.
450 Micrographs of the cellular periphery of strain M1^T cells imaged at different magnifications.

451

452 **Figure 2.** Maximum likelihood phylogenetic tree based on 16S rRNA gene sequences of
453 *Oxyplasma meridianum* M1^T and its closest phylogenetic neighbours with validly published names.
454 Bootstrap values are based on 1,000 replicates and those <80 are shown as open circles, values >80
455 as closed circles. Sequences were previously aligned using MAFFT v7 and the resulting multiple
456 alignment was trimmed using TrimAl 1.2rev59. The tree was constructed and decorated under R
457 programming environment using the package phangorn for the tree calculations, selecting
458 TIM3+I+G as best substitution model (using ModelTest plugin within phangorn) and stochastic
459 algorithm for tree rearrangement.

460

461 **Figure 3.** Phylogenetic tree based on 122 concatenated proteins. Tree calculation was performed
462 using the GTDB-tk tool focusing exclusively on the *Thermoplasmatales* order, using genus
463 *Aciduliprofundum* as an outgroup. Bootstrap values are highlighted as closed circles (values > 80),
464 and open circles (bootstrap values <80).

465

466